Available online at www.sciencedirect.com
SCIENCE DIRECT
Journal of Power Sources 154 (2006) 8–17
JOURNAL OF POWER SOURCES
www.elsevier.com/locate/jpowsour

Evaluation of the thickness of membrane and gas diffusion layer with simplified two-dimensional reaction and flow analysis of polymer electrolyte fuel cell

Gen Inoue *, Yosuke Matsukuma, Masaki Minemoto

Department of Chemical Engineering, Faculty of Engineering, Kyushu University, Hakozaki, Higashi-ku, Fukuoka 812-8581, Japan

Received 26 November 2004; received in revised form 4 March 2005; accepted 25 March 2005
Available online 6 June 2005

Abstract

In the development of more efficient and stable polymer electrolyte fuel cell (PEFC), it is important to propose the optimal component shape that can generate high power and uniform the current density distribution in a single cell. In this study, our past model was improved, and simplified two-dimensional PEFC analysis model including flow and heat transfer of cooling water was made. And PEFC internal phenomenon, that is hardly measured experimentally, could be examined by using this model. The influence of changing the thickness of membrane and gas diffusion layer (GDL) on the cell performance was calculated. As a result, it was confirmed that it is possible to improve the cell output by thinning the GDL more than the membrane in case of low voltage and by thinning the membrane more than the GDL in case of high voltage, but thinning the membrane and the gas diffusion layer increased the current density distribution. In addition, by arranging the values of average current density and the current density distribution, the evaluation graphs were made, which became a help of the shape design in the membrane and the gas diffusion layer.

Keywords: PEFC; Numerical analysis; Current density distribution; Relative humidity distribution; Membrane; Gas diffusion layer

1. Introduction

Now, fuel cells are developed from the viewpoint of the effective utilization of energy and the protection of the environment. Especially, polymer electrolyte fuel cell (PEFC) is expected as driving power of vehicles and stationary power supply. And the performance of PEFC is greatly improved because of development of new component and optimization of the system. As the PEFC power generation characteristic is affected by the structure, the material, and the operating condition, it is greatly important to understand the correlation mechanism of a complex physicochemical phenomenon in the cell in detail. But there are hardly any researches that examine PEFC internal phenomenon while electricity is generated. As it is very difficult to measure accurately the current density distribution and relative humidity distribution in experiments, the numerical analysis is an effective method to examine them. On the other hand, PEFC is demanded to have long life and high durability, and the longevity examination is often carried out. However, the accelerated test of PEFC is difficult because neither the deterioration factor nor the mechanism is clear. It is thought that the numerical analysis can be applied to the investigation of such degradation factor and mechanism. Bernardi and Verbrugge [1,2] and Springer et al. [3] developed one-dimensional model to the direction of membrane thickness, and examined concentration distribution and water management in PEFC. Fuller and Newman [4] analyzed developed two-dimensional model to the direction of membrane thickness and gas flow channel. Nguyen and White [5], and Yi and Nguyen [6] developed heat and water transport models (2-D) that accounted for various operation condition and membrane hydration conditions. On the other hand, it is thought that analysis with the

* Corresponding author. Tel.: +81 92 642 3523; fax: +81 92 642 3523.
E-mail address: ginoue@chem-eng.kyushu-u.ac.jp (G. Inoue).

0378-7753/$ – see front matter © 2005 Elsevier B.V. All rights reserved.
doi:10.1016/j.jpowsour.2005.03.218

Nomenclature

b_c	condensation rate constant ($1\,s^{-1}$)
C_j	molar concentration of species j ($mol\,m^{-3}$)
C_p	specific heat at constant pressure ($J\,(kg\,K)^{-1}$)
$E_{\Delta H}$	the value of reduction change of water enthalpy to voltage (V)
F	Faraday's constant ($96485\,C\,mol^{-1}$)
h	heat transfer coefficient of gas ($J\,(m^2\,s\,K)^{-1}$)
h_w	heat transfer coefficient of cooling water ($J\,(m^2\,s\,K)^{-1}$)
ΔH_{H_2O}	change of water enthalpy between vapor and liquid ($J\,mol^{-1}$)
i	current density ($A\,m^{-2}$)
k	thermal conductivity of solid phase ($J\,(m\,s\,K)^{-1}$)
k^{sep}	thermal conductivity of separator ($J\,(m\,s\,K)^{-1}$)
l_d	GDL thickness (m)
l_g	gas channel depth (m)
l_w	cooling water groove depth (m)
l^s	thickness of solid phase (m)
l^{sep}	separator thickness between cooling water and gas phase (m)
M_j	molecular weight of species j ($kg\,mol^{-1}$)
p	pressure in Eq. (3) (Pa)
$P_{H_2O,sat}$	saturated vapor pressure in stream (Pa)
q_1	heat flux from solid phase to gas phase ($J\,(m^2\,s)^{-1}$)
q_2	heat flux from cooling water to gas phase ($J\,(m^2\,s)^{-1}$)
q_3	heat value generated by reaction ($J\,(m^2\,s)^{-1}$)
q_4	heat flux from gas phase to solid phase ($J\,(m^2\,s)^{-1}$)
q_5	heat flux from cooling water to solid phase ($J\,(m^2\,s)^{-1}$)
q_6	latent heat value of condensation ($J\,(m^2\,s)^{-1}$)
$q_{w(1)}$	heat flux from gas phase to cooling water ($J\,(m^2\,s)^{-1}$)
$q_{w(2)}$	heat flux from solid phase to cooling water ($J\,(m^2\,s)^{-1}$)
r_j	molar flux of species j ($mol\,(m^2\,s)^{-1}$)
R	gas constant ($8.314\,J\,(mol\,K)^{-1}$)
R_{rea}	all reaction rate ($1\,s^{-1}$)
t	time (s)
t_m	membrane thickness (m)
T	gas phase temperature (K)
T_w	cooling water temperature (K)
T^s	solid phase temperature (K)
U	overall heat transfer coefficient between gas and cooling water ($J\,(m^2\,s\,K)^{-1}$)
U^s	overall heat transfer coefficient between cooling water and solid phase ($J\,(m^2\,s\,K)^{-1}$)
v	flow velocity ($m\,s^{-1}$)
V	operation voltage (V)
x	distance (m)
Δx	distance on calculation mesh to neighboring gas channel (m)

Greek letters

α	net water transfer coefficient
ρ	density of mixture ($kg\,m^{-3}$)

Subscripts

j	species j
w	cooling water

Superscripts

a	anode
c	cathode
k	anode or cathode
s	solid phase
sep	separator

computational fluid dynamics (CFD) technique is important in order to calculate the transport phenomena in detail, and such study is increasing recently. Um et al. [7] and Wang et al. [8] have developed two-dimensional model with CFD, which included two-phase flow. Dutta et al. [9] made a three-dimensional computational model based on the commercial software package Fluent. Berning et al. [10] presented a non-isothermal, three-dimensional models and calculated the distribution of current density and concentration in the straight channel. Mazumder and Cole [11] examined the liquid water transport with three-dimensional model. Li et al. [12] analyzed in small cell with three-dimensional analysis. Um and Wang [13] compared the performance of straight flow channel with that of interdigiteted flow channel by three-dimensional analysis. Berning and Djilali [14] examined the effect of the porosity and thickness of gas diffusion layer in straight channel with three-dimensional model. These PEFC numerical analysis models contributed to the optimization of component design and operation condition, and to the examination of issues included in present cell. However, these studies calculated internal phenomena in short straight gas channel and one serpentine channel or in small cell, and there are very few researches that evaluated various component shapes of actual size cell under considering realistic calculation time and calculation resource.

In our past researches [15], the effects of changing operation temperature, humidify temperature and hydrogen and oxygen concentration in supply gas on the *I–V* characteristic of a small PEFC were examined experimentally. For the experiment, we developed two models: one was PEFC reaction model that could show these influences on PEFC reaction characteristics; the other was PEFC reaction and flow analysis model that was combined with the thermal flow analysis. With this PEFC reaction and flow analysis model, five kinds of separators were evaluated from the viewpoint of gas flow condition, uniformity of current density and tem-

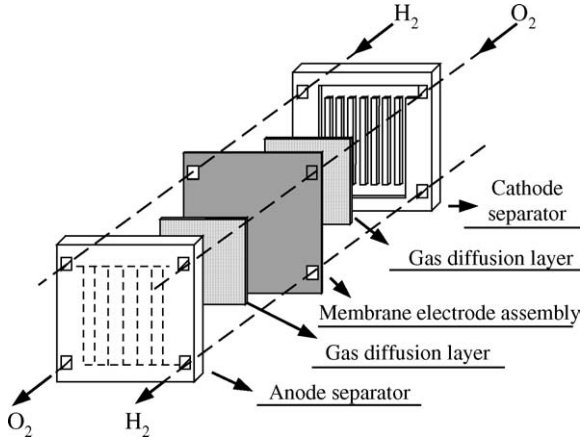

Fig. 1. Schematic diagram of PEFC single cell.

perature, reduction of pressure drop, and ejection of water. In this study, we made a new simplified PEFC analysis model that included the flow and heat transfer of cooling water, and examined the influence of membrane and gas diffusion layer thickness on cell performance with this model.

As the gas diffusion layer (GDL), which is a component of PEFC is thinner, the concentration overvoltage is lower, because the diffusion length becomes short. And the thinner electrolyte membrane is, the lower the resistance overvoltage is, because the ion transfer length becomes short. Consequently, GDL and electrolyte membrane were expected to be thin in order to reduce the cell voltage drop. (Actually, those thicknesses were limited by the viewpoint of strength, manufacture, etc.) On the other hand, from the viewpoint of durability of catalyst and membrane, it is expected that the current density distribution and relative humidity distribution become uniform in overall cell. In this study with numerical analysis method, the effect of thickness of GDL and membrane was examined from the following two view points; one was the achievement of high out put density, and the other was the formation of uniform current density distribution and uniform relative humidity distribution.

2. Simplified reaction and flow analysis of PEFC

2.1. Structure of PEFC analysis model

Fig. 1 shows schematic of PEFC single cell that is object in this study. PEFC consists of a membrane electrode assembly (MEA), two gas diffusion layers (GDL) and two separators. Polymer membrane of MEA has proton conductivity and is sandwiched between two thin platinum electrode layers. MEA is sandwiched between two GDL and two separators. Table 1 shows the specification of MEA, GDL, and the separator targeted in this study. The flow channel shape of the separator was variously developed. In this study, we used only the serpentine separator shown in Fig. 2. The electrode area was a square with 150 mm side. Fifteen channels, which have

Table 1
Specification of this PEFC

MEA	
Thickness of membrane	30, 50, 100 μm
Size of catalyst layer	150 mm × 150 mm
Amount of Pt	3.0 g m^{-2}
GDL	
Size	150 mm × 150 mm
Thickness	300 μm
Separator	
Number of the channel	15
Channel width	1 mm
Shoulder width	1 mm
Channel depth	0.5 mm

1 mm groove width and shoulder width and 0.5 mm groove depth, turned four times. Anode gas and cathode gas were counter flow. Cooling water flowed in the back of the separator, and the channel shape was the same as the gas separator. The anode gas (hydrogen 75% and nitrogen 25% as reforming gas) and the cathode gas (oxygen 21% and nitrogen 79% as air) were supplied to the cell, respectively. The supply gases flowed through the humidifier set up on the upstream of the cell, operating the humidifier temperature to control the humidity. The inlet gas flow rate was set automatically by hydrogen utilization, oxygen utilization and average current density. The inlet cooling water flow rate was set so that the temperature of outlet cooling water can become preset value.

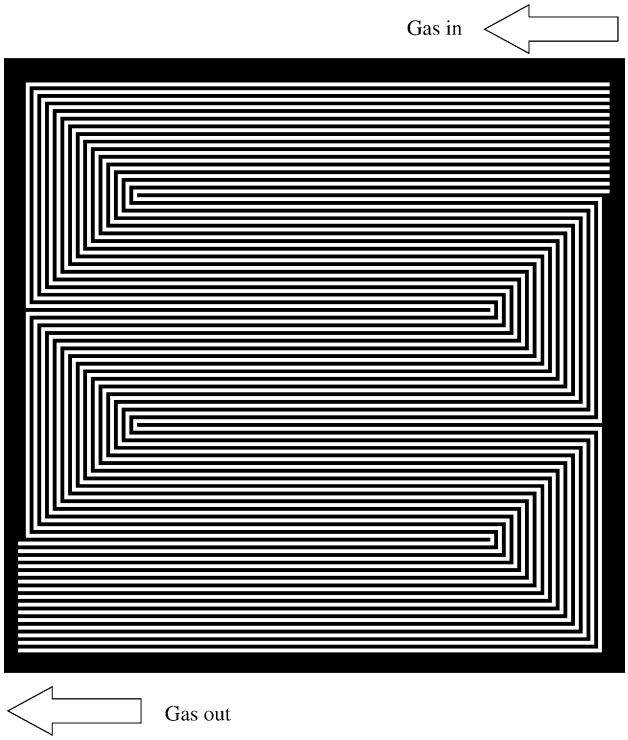

Fig. 2. Gas channel shape of separator.

2.2. Model development and assumption

First, the most important point of this model explanation was shown as followings. The various PEFC numerical analysis models, which were explained in Introduction in details, were developed up to the present. These analysis models were summarized in followings. First, one-dimensional model of the direction across the membrane was developed. Next, two-dimensional model was developed by adding the direction along the gas channel to one-dimensional model. And then, three-dimensional model was developed by adding the direction of across the gas channel. On the other hand, Nguyen and White [5], and Yi and Nguyen [6] did not consider the water distribution across the membrane on the assumption that the membrane, catalyst layer and gas diffusion layer were too thin. And they assumed that the membrane, catalyst layer and gas diffusion layer were unified homogeneously and calculated the local current density and water transfer coefficient by using the local concentration and the temperature, which corresponded to the local current density point, in both of anode and cathode gas channels. The direction across the membrane of our model was based on the Nguyen's model and was developed on the assumption that the membrane, catalyst layer and gas diffusion layer were unified homogeneously and the local current density and water transfer coefficient was calculated from the local concentration and the temperature in gas channel. The direction along gas channel of Nguyen's model was the plug flow model, and the shape of this model was changed from the straight shape to the meander shape in this paper. Therefore the gas flow direction was extended to the direction of parallel to membrane (x, y-direction). In the microscopic part including the direction across the membrane, our model may be not as accurate as other three-dimensional models. But, the calculation speed became faster and the calculation resources became fewer than other models by simplifying. That is why it became possible to calculate the influence on overall cell in an actual size cell with our model, even though it is difficult to calculate that with other three-dimensional detailed model. Therefore our model is very effective to examine the overall cell tendency in an actual size cell, though the calculation of the membrane thickness direction was sacrificed.

As stated above, one-dimension expresses the direction along gas channel (x direction), and two-dimension expresses the direction of membrane plane, which included x direction and the direction across the gas channel (x–y direction). However, in the figure of current density distribution and relative humidity distribution, x and y-axes were converted to rectangular coordinate in order to help to understand easily.

So far we have been examining the PEFC reaction and flow analysis. In this study, we improved the former model and developed the new model that could be used for real cell calculation in detail.

Fig. 3 shows the PEFC simulation model. As shown in this figure, gas flow velocity, concentration and temperature were calculated in the gas channel on the anode and cathode. And it was assumed that the temperature distributions of MEA and GDL were same as each other, and that they were unified, the temperature and current density were calculated in it. (This unified part is expressed as the solid phase.) The governing equations in this simulation were derived with the following assumption.

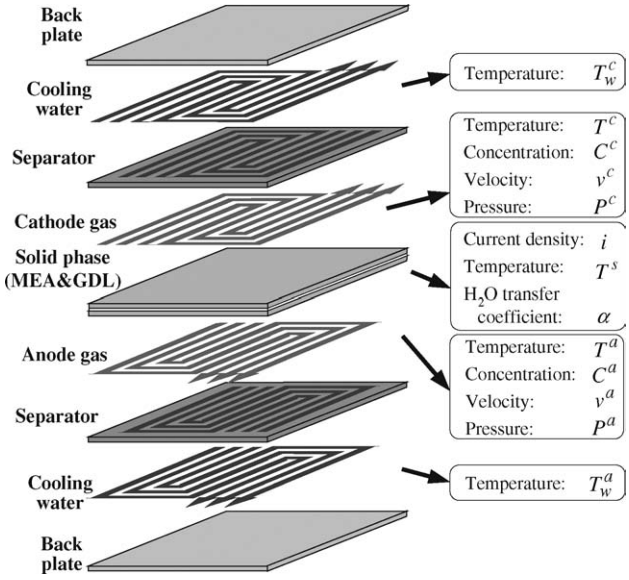

Fig. 3. Model for the simulation of the PEFC.

1. The gas flows uniformly in each channel of the separator. Similarly, the cooling water flows uniformly.
2. The volume of the condensation water is ignored, and the water moves with the gas.
3. The reaction area reduction caused by flooding of electrode is ignored, and the diffusion prevention caused by water condensation is ignored.
4. Fluid is incompressible Newtonian fluid and ideal gas. Flow condition is laminar flow.
5. Heat transfer between separator and gas is ignored. But heat transfer between gas phase, solid phase and cooling water is included.
6. Cell voltage is uniform and constant.
7. Only resistance overvoltage and water transfer in membrane include influence of temperature.
8. In membrane, ionic conductivity, electro osmosis coefficient and water effective diffusion coefficient that depend on membrane humidity are determined by water activity of anode side.
9. The membrane thickness and GDL thickness correspond to the migration length of the proton and water in membrane, and to the diffusion length in GDL, respectively. And physical and electrochemical properties of the membrane and GDL are equal in any shape.
10. The gas crossover is disregarded.

2.3. Derivation of simplified PEFC analytical model

In our past method [15], in order to calculate the gas flow rate distribution in each channel, two-dimensional analysis model was used. In this study, One-dimensional analysis as plug flow in each channel was available because of the assumption that the gas flow rate distribution was uniform. Though the separator shape was two-dimension structure to the direction of the membrane face, the quasi-two-dimension analysis model was made by assuming the direction from the inlet to the outlet to be a positive x-direction in each channel and by making the channel meander. As a result, the simplification of the equations and the speed-up of the calculation became possible. However, in case of calculation of the solid phase temperature distribution, it was calculated by two-dimensional analysis model. Moreover, for the simplification of the calculation, these three terms following were ignored: the viscous term in the motion equations; the heat conduction term in the energy balance equations; the diffusion term in the mass balance equations.

The equation of continuity is shown by the following expression

$$\frac{\partial v^{\mathrm{k}}}{\partial x} = -R^{\mathrm{k}}_{\mathrm{rea}} \tag{1}$$

where v is the velocity of mixed gas, x is distance along the gas flow channel, R_{rea} is all reaction rate, and the superscript k is the anode side or the cathode side. R_{rea} is calculated by the following equation

$$R^{\mathrm{k}}_{\mathrm{rea}} = \frac{1}{l^{\mathrm{k}}_{\mathrm{g}}\rho^{\mathrm{k}}}\sum_j M_j r^{\mathrm{k}}_j \tag{2}$$

where l_{g} is the depth of gas channel, ρ is the density of mixed gas, M_j is the molecular weight of chemical species j, r_j is the reaction or condensation rate per unit area of chemical species j.

The equation of motion is shown by the following expression

$$\rho^{\mathrm{k}}\frac{Dv^{\mathrm{k}}}{Dt} = -\nabla p^{\mathrm{k}} + \rho^{\mathrm{k}} v^{\mathrm{k}} R^{\mathrm{k}}_{\mathrm{rea}} \tag{3}$$

where p is pressure, and the operator D/Dt is substantial time derivative that is shown by the following expression

$$\frac{Dv^{\mathrm{k}}}{Dt} = \frac{\partial v^{\mathrm{k}}}{\partial t} + v^{\mathrm{k}}\frac{\partial v^{\mathrm{k}}}{\partial x} \tag{4}$$

The equation of chemical species j is shown by the following expression

$$\frac{DC^{\mathrm{k}}_j}{Dt} = -\frac{r^{\mathrm{k}}_j}{l^{\mathrm{k}}_{\mathrm{g}}} + C^{\mathrm{k}}_j R^{\mathrm{k}}_{\mathrm{rea}} \tag{5}$$

where C_j is the concentration of chemical species j. The equations of species were derived to eight kinds of $C^{\mathrm{a}}_{\mathrm{H_2}}$, $C^{\mathrm{a}}_{\mathrm{N_2}}$, $C^{\mathrm{a}}_{\mathrm{H_2O(v)}}$, $C^{\mathrm{a}}_{\mathrm{H_2O(l)}}$, $C^{\mathrm{c}}_{\mathrm{O_2}}$, $C^{\mathrm{c}}_{\mathrm{N_2}}$, $C^{\mathrm{c}}_{\mathrm{H_2O(v)}}$, $C^{\mathrm{c}}_{\mathrm{H_2O(l)}}$ that are hydrogen, oxygen, nitrogen, vapor and condensed water in anode and cathode channel.

The equations of energy are shown by the following expressions

$$\text{(Gas)}\quad \rho^{\mathrm{k}} C^{\mathrm{k}}_{\mathrm{p}}\frac{DT^{\mathrm{k}}}{Dt} = \frac{q^{\mathrm{k}}_1 + q^{\mathrm{k}}_2}{l^{\mathrm{k}}_{\mathrm{g}}} + \rho^{\mathrm{k}} C^{\mathrm{k}}_{\mathrm{p}} T^{\mathrm{k}} R^{\mathrm{k}}_{\mathrm{rea}} \tag{6}$$

$$\text{(Solid)}\quad \rho^{\mathrm{s}} C^{\mathrm{s}}_{\mathrm{p}}\frac{\partial T^{\mathrm{s}}}{\partial t} = k^{\mathrm{s}}\nabla^2 T^{\mathrm{s}} + \frac{q^{\mathrm{s}}_3 + q^{\mathrm{s}}_4 + q^{\mathrm{s}}_5 + q^{\mathrm{s}}_6}{l^{\mathrm{s}}} \tag{7}$$

$$\text{(Cooling water)}\quad \rho_{\mathrm{w}} C_{\mathrm{p(w)}}\frac{DT^{\mathrm{k}}_{\mathrm{w}}}{Dt} = \frac{q^{\mathrm{k}}_{\mathrm{w(1)}} + q^{\mathrm{k}}_{\mathrm{w(2)}}}{l^{\mathrm{k}}_{\mathrm{w}}} \tag{8}$$

In the energy equation of gas, C_p is specific heat, T is temperature, q_1 and q_2 are heat fluxes from solid phase and cooling water, respectively. In the equation of solid phase, k is heat conductivity, l^{s} is the thickness of solid phase, q_3 is the heat value per unit area the result of electrochemical reaction, q_4 and q_5 are heat fluxes from gas and cooling water, respectively, q_6 is latent heat flux of water condensation, and the superscript s is solid phase. In the equation of cooling water, l_{w} is the depth of cooling water channel, $q_{\mathrm{w(1)}}$ and $q_{\mathrm{w(2)}}$ are heat fluxes from gas and solid phase, respectively, and the subscript w is cooling water. These heat flux and heating value are shown by the following equation

$$\begin{aligned}
q^{\mathrm{k}}_1 &= h^{\mathrm{k}}(T^{\mathrm{s}} - T^{\mathrm{k}}), \qquad q^{\mathrm{k}}_2 = U^{\mathrm{k}}(T^{\mathrm{k}}_{\mathrm{w}} - T^{\mathrm{k}}),\\
q^{\mathrm{s}}_3 &= (E_{\Delta H} - V)i, \qquad q^{\mathrm{s}}_4 = h^{\mathrm{a}}(T^{\mathrm{a}} - T^{\mathrm{s}}) + h^{\mathrm{c}}(T^{\mathrm{c}} - T^{\mathrm{s}}),\\
q^{\mathrm{s}}_5 &= U^{\mathrm{s(a)}}(T^{\mathrm{a}}_{\mathrm{w}} - T^{\mathrm{s}}) + U^{\mathrm{s(c)}}(T^{\mathrm{c}}_{\mathrm{w}} - T^{\mathrm{s}}),\\
q^{\mathrm{s}}_6 &= -\Delta H_{\mathrm{H_2O}}(r^{\mathrm{a}}_{\mathrm{H_2O(l)}} + r^{\mathrm{c}}_{\mathrm{H_2O(l)}}),\\
q^{\mathrm{k}}_{\mathrm{w(1)}} &= U^{\mathrm{k}}(T^{\mathrm{k}} - T^{\mathrm{k}}_{\mathrm{w}}), \qquad q^{\mathrm{k}}_{\mathrm{w(2)}} = U^{\mathrm{s(k)}}(T^{\mathrm{s}} - T^{\mathrm{k}}_{\mathrm{w}})
\end{aligned} \tag{9}$$

where h is heat transfer coefficient of anode or cathode gas, $E_{\Delta H}$ is the value of reduction change of water enthalpy to voltage, V is voltage, i is current density, $\Delta H_{\mathrm{H_2O}}$ is change of water enthalpy between vapor and liquid, U^{k} is overall heat transfer coefficient between anode gas or cathode gas and cooling water, $U^{\mathrm{s(k)}}$ is overall heat transfer coefficient between anode or cathode side cooling water and solid phase. These overall heat transfer coefficients are shown by following equations

$$\begin{aligned}
U^{\mathrm{k}} &= \frac{1}{(1/h^{\mathrm{k}}) + (l^{\mathrm{sep}}/k^{\mathrm{sep}}) + (1/h^{\mathrm{k}}_{\mathrm{w}})},\\
U^{\mathrm{s(k)}} &= \frac{1}{((l^{\mathrm{sep}} + l^{\mathrm{k}}_{\mathrm{g}})/k^{\mathrm{sep}}) + (1/h^{\mathrm{k}}_{\mathrm{w}})}
\end{aligned} \tag{10}$$

where l^{sep} is separator thickness between cooling water and gas phase, k^{sep} is heat conductivity of separator, $h^{\mathrm{k}}_{\mathrm{w}}$ is heat transfer of cooling water of anode side or cathode side.

The reaction and condensation rates of each ingredient are shown by the following equation

$$r^{a}_{H_2} = \frac{i}{2F}, \quad r^{a}_{H_2O(v)} = \alpha\frac{i}{F} + l^{a}_{g}b_c\left(C^{a}_{H_2O(v)} - \frac{P^{a}_{H_2O,sat}}{RT^{a}}\right),$$

$$r^{a}_{N_2} = 0, \quad r^{a}_{H_2O(l)} = -l^{a}_{g}b_c\left(C^{a}_{H_2O(v)} - \frac{P^{a}_{H_2O,sat}}{RT^{a}}\right),$$

$$r^{c}_{O_2} = \frac{i}{4F}, \quad r^{c}_{H_2O(v)} = -(1+2\alpha)\frac{i}{2F} + l^{c}_{g}b_c\left(C^{c}_{H_2O(v)} - \frac{P^{c}_{H_2O,sat}}{RT^{c}}\right),$$

$$r^{c}_{N_2} = 0, \quad r^{c}_{H_2O(l)} = -l^{c}_{g}b_c\left(C^{c}_{H_2O(v)} - \frac{P^{c}_{H_2O,sat}}{RT^{c}}\right) \quad (11)$$

where F is Faraday's constant, R is gas constant, $P_{H_2O,sat}$ is saturated vapor pressure, α is water transfer coefficient, b_c is condensation rate constant.

Current density i was calculated with PEFC reaction model that authors built in past study [15]. The electromotive force, the resistance overvoltage, the activation overvoltage, and the concentration overvoltage were modeled from theoretical equations, respectively. On the other hand, small PEFC with single gas channel was made, which was not much affected by the gas flow condition and the concentration distribution, and the effects of changing the concentration of the supply gas, the temperature of the cell, the humidifier temperature, the gas mass flow, and the gas channel length were investigated by the power generation examination of this cell. By comparing the experimental results with the calculation results in all operation condition, the parameters of the model equations were decided with the trial and error method. And the calculation data was able to agree with the experimental data by using those parameters. In this model, the current density was calculated by the following equation as the function of local concentration and temperature.

$$i = f(V, C^{a}_{H_2}, C^{a}_{H_2O(v)}, C^{c}_{O_2}, C^{c}_{H_2O(v)}, T^{a}, T^{c}, T^{s}) \quad (12)$$

As an example, when the concentration of oxygen in the cathode supply gas was changed, the comparison between the experimental data and the calculation data of current density–voltage curve is shown in Fig. 4. The experimental data and the calculation data agreed with each other on all conditions. Similarly, it was confirmed that the *I–V* curve was predictable for other conditions with this model.

It is thought that water is moved with two mechanisms of electro osmosis and back diffusion in the electrolyte membrane. When one proton moves from the anode side to the cathode side, the water movement coefficient α shows the net number of water molecules moving along with proton. This is from the method by Nguyen and White [5].

Eqs. (1)–(12) are connected in their respective group, such as reaction, concentration, temperature and flow, and their partial differential equations are discretized by finite differential method. The boundary conditions of flow velocity, temperature, and concentration are set as followings:

(1) gas inlet boundary: these variables are constant,
(2) gas outlet boundary: the gradients of these variables are constant.

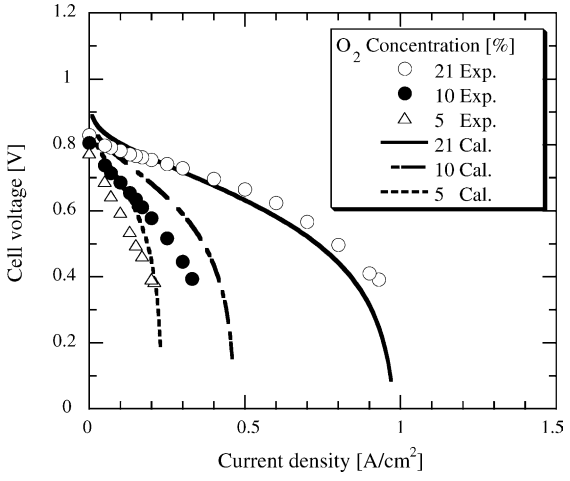

Fig. 4. Effect of O_2 concentration on cell voltage–current density plots with experimental and calculated results.

Current density and water transfer coefficient were calculated all over the electrode area. In case of calculation of these variables at gas channel area, the local concentration and temperature at that point were used as the needed variables. In case of calculation of these variables at no gas channel area (at shoulder area), the local values at adjoining gas channel were used. In this case, the diffusion length l_d was changed to $\sqrt{(l_d)^2 + (\Delta x)^2}$ in equation that calculates the limiting current density, and gas diffusibility to shoulder area was considered. Δx is the width of calculation mesh. And the reaction rate of this shoulder area was put in the balance equations of adjoining mesh point at gas channel, and the conservation low was satisfied in single cell. Those variables were calculated until becoming stationary state. The relative errors of balance equation of mass, species and energy became 1% or less in all the calculations. Table 2 shows the calculation system and method used in this study.

3. Results and discussions

In general, thinning membrane and GDL is effective in the decrease of the resistance overvoltage and concentration

Table 2
Calculation system and method used in this study

Analysis dimension	One-dimension
Coordinate system	Rectangular coordinates
Digitization of space	Finite difference method
Handing of convection term	QUICKER method
Making time dispersed	Euler scheme
Flow analysis algorithm	FS method
Iteration of pressure	SOR method
Mesh	Square staggered mesh 150×150

Table 3
Operation conditions

Pressure	0.1 MPa
Inlet gas temperature	70 °C
Inlet cooling water temperature	70 °C
Outlet cooling water temperature	75 °C
Humidify temperature	60, 70 °C
Operation voltage	0.5, 0.6, 0.7 V
Utilization rate	
H_2	75%
O_2	40%
Inlet gas composition	
Anode	H_2, 75.0%
	N_2, 25.0%
Cathode	O_2, 21.0%
	N_2, 79.0%

overvoltage, respectively. But, it has not been examined how these influence on internal phenomenon of a real cell. Consequently, in this study, we examined the influence of MEA and GDL thickness on current density distribution, relative humidity distribution, and cell performance with a model that can calculate. Table 3 shows operation condition. Fig. 5 shows the current density distribution in case of the membrane thickness being changed on 0.7 V, and Fig. 6 shows the anode relative humidity distribution. The solid line arrows show the inlet and the outlet of cathode gas, the broken arrows show the inlet and the outlet of anode gas in Figs. 5 and 6. In Fig. 5, as the membrane thickness increased, the current density decreased because of the increase of resistance overvoltage. And the position of the high current density and the low current density changed. In case of 30 μm membrane, because of the concentration overvoltage, the current density was high in the upstream of the anode and cathode channel, and it was

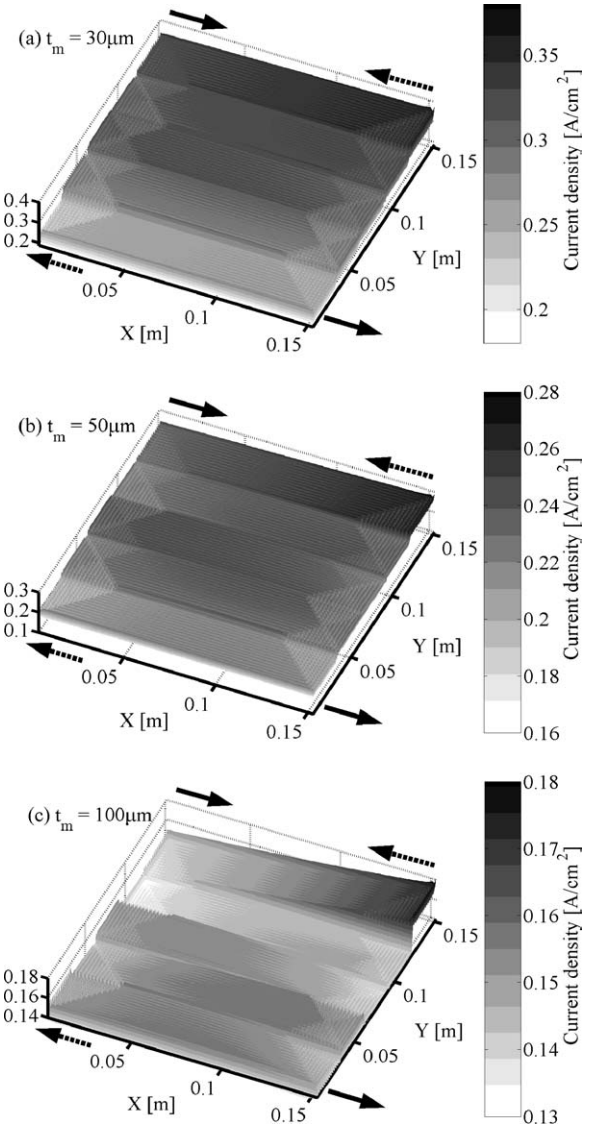

Fig. 5. Effect of thickness of membrane on current density distribution at 0.7 V (average current density (a): 0.276 A cm^{-2}, (b): 0.221 A cm^{-2}, (c): 0.146 A cm^{-2}).

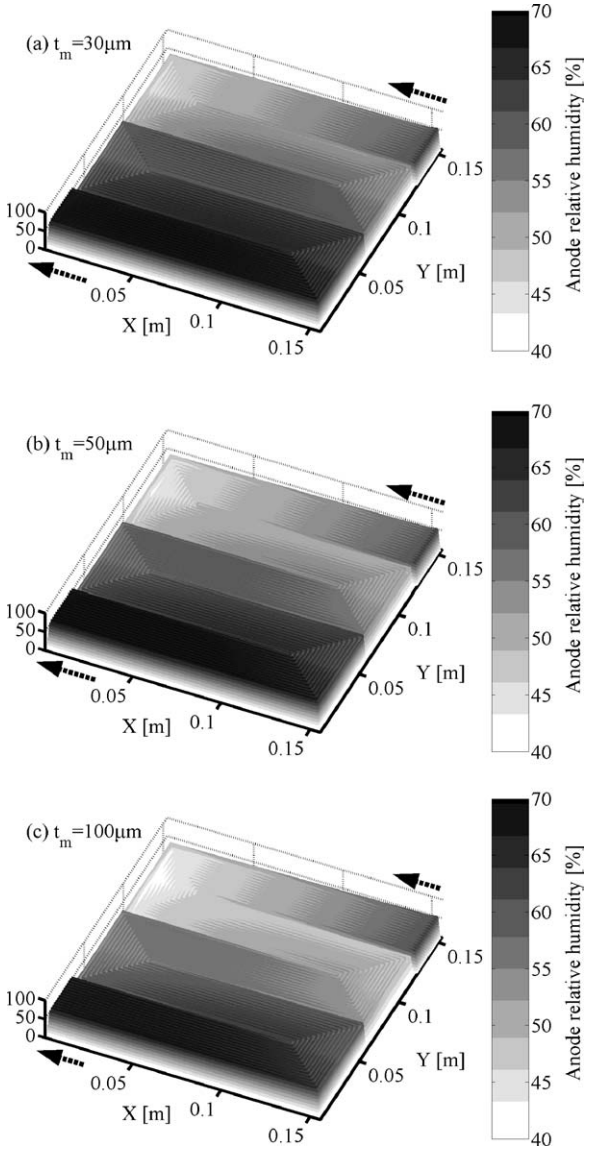

Fig. 6. Anode relative humidity distribution at 0.7 V.

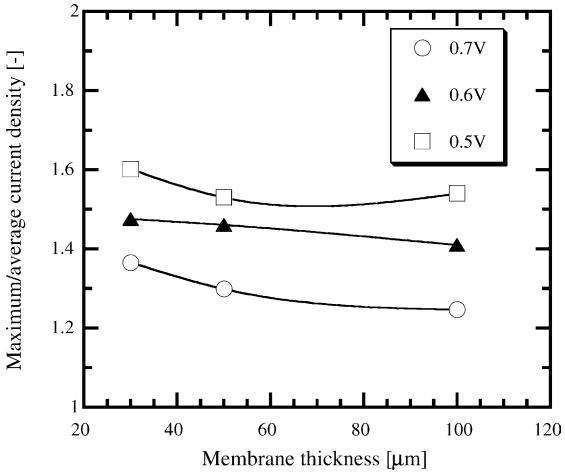

Fig. 7. Relationship between membrane thickness and maximum/average of current density.

low in the downstream. In case of 50 μm membrane, because the influence of the resistance overvoltage increased, the current density was high at the position of the inlet where the anode vapor concentration was high. In the place where the anode gas flowed from inlet a little, the anode vapor concentration decreased by the electro-osmosis effect, and the current density decreased. However, at the position from the middle reached to the downstream, because of the back diffusion from the cathode, the anode vapor concentration was high, and the current density rose gradually. This tendency was more remarkable in case of 100 μm membrane. It was possible to confirm these things from the anode side relative humidity distribution of Figs. 6 and 7 shows the influence of the membrane thickness on the ratio between the maximum current density and the average current density (maximum current density/average current density). The rate was increasing by thinning the membrane, and this caused like following. In case of thin membrane, though the current density was high on the upstream because of the decrease in the resistance overvoltage and the maintenance of anode humidity. On the other hand, the current density was low on the downstream because of the decrease in the oxygen concentration that results from the consumption for reaction. Moreover, as the voltage lowers, the influence of the membrane thickness on the current density distribution became small because the concentration overvoltage increased. Because the increase of the current density distribution influences on local degradation and the durability of the membrane, it is necessary to decrease this distribution. Accordingly, it is important to design the cell having high power density and uniform current density distribution as much as possible. Fig. 8 shows the influence of the membrane thickness on the ratio between the cathode relative humidity and the anode relative humidity (cathode relative humidity/anode relative humidity). By the

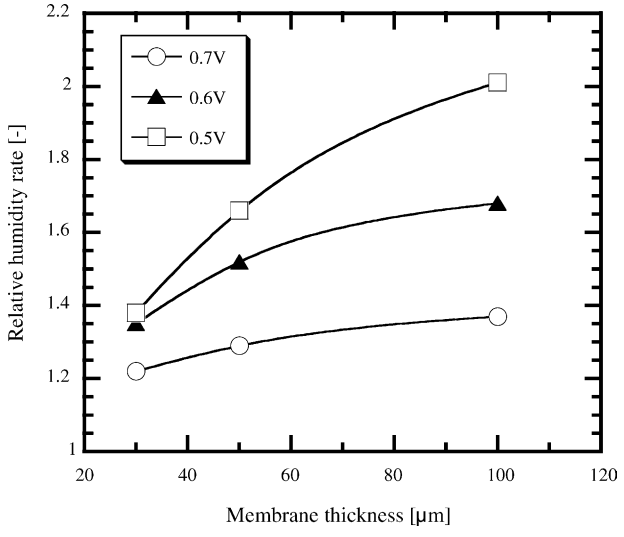

Fig. 8. Relationship between membrane thickness and the relative humidity ratio of anode and cathode.

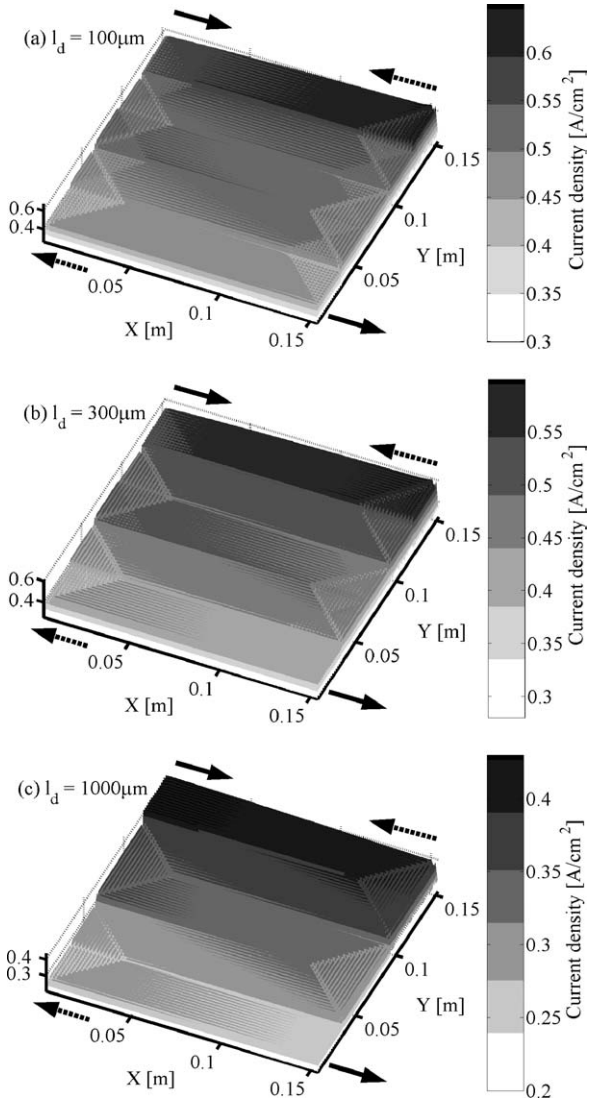

Fig. 9. Effect of thickness of GDL on current density distribution at 0.5 V (average current density (a): 0.434 A cm^{-2}, (b): 0.415 A cm^{-2}, (c): 0.305 A cm^{-2}).

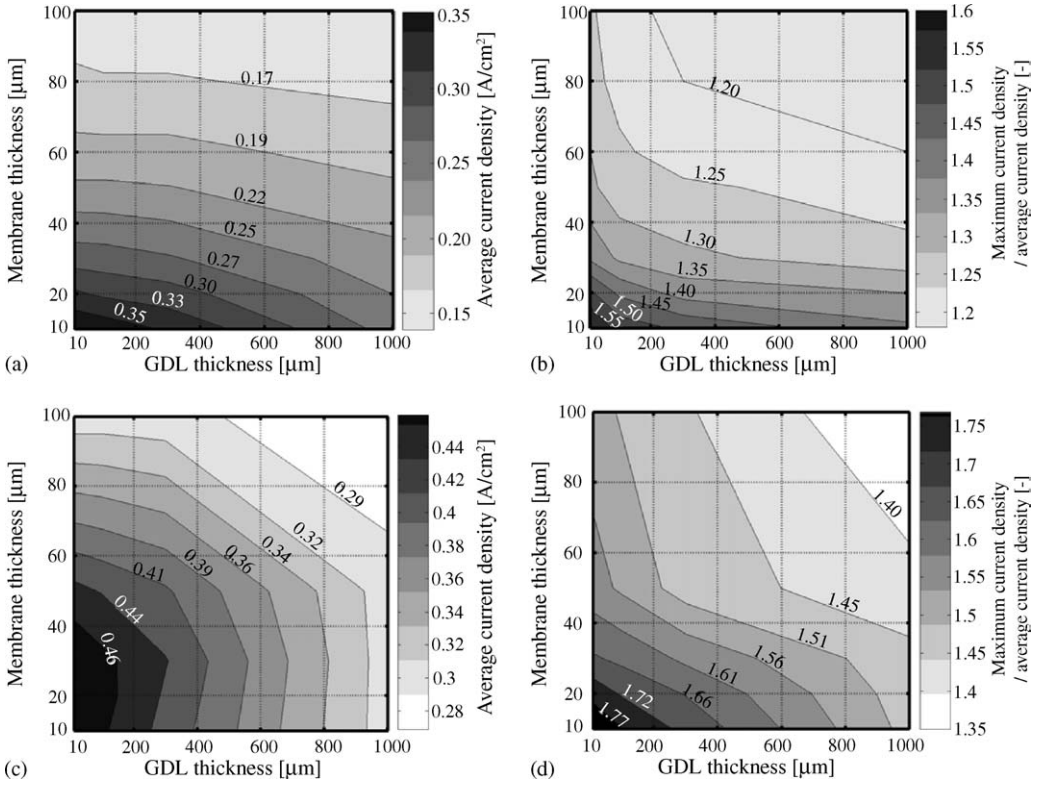

Fig. 10. Effects of membrane and GDL thickness on average current density and current density distribution at 0.5 V and 0.7 V: (a) average current density at 0.7 V, (b) current density distribution at 0.7 V (c) average current density at 0.5 V, (d) current density distribution at 0.5 V.

drop of voltage, this ratio increased, because the amount of the water generation and electro-osmosis increased. Moreover, in case of thick membrane, this ratio increases because the amount of back diffusion of water decreased.

Next, the influence of the GDL thickness was examined by the calculation. Fig. 9 shows the current density distribution in case GDL thickness is changed at 0.5 V. The solid line arrows show the inlet and the outlet of cathode gas, the broken arrows show the inlet and the outlet of anode gas in this figure. The concentration overvoltage decreased by thinning the GDL thickness, and the current density increases all over the cell. Moreover in the low voltage, the current density decreased along the cathode gas flow pattern because the influence of oxygen concentration overvoltage was strong.

Next, the above calculation result of changing the membrane thickness and the GDL thickness was arranged. Fig. 10 is the evaluation graph of the membrane thickness and the GDL thickness concerning average current density and current density distribution. Comparing Fig. 10(a), which is average current density at 0.7 V, with (c), which is average current density at 0.5 V, it was confirmed that the cell output could be improved by thinning the GDL more than the membrane in case of low voltage and by thinning the membrane more than the GDL in case of high voltage. Moreover, these evaluation graphs could be applied to design the PEFC components. For example, in case of development of the satisfying cell the requirement, that the average current density is larger than a certain value, and that the current density distribution is smaller than a certain value, with these evaluation graphs, it can be decided that the size of membrane and GDL in intersection of two areas where those conditions are satisfied is the best. Fig. 10 is the result only about the influence of the shape of the electrolyte membrane and the GDL to the average current density and current density distribution. As there are many kinds of the operating condition of PEFC, (for example cell and gas temperature, humidification condition, component of inlet gas, hydrogen and oxygen utilization, operating voltage, and pressure), it is difficult to examine in all these operation condition and to arrange these results. The specific best shape of membrane and GDL could not be described still in this study. However, it was thought that the course for the best design of the PEFC component could be obtained by calculating in various conditions by this PEFC numerical analysis model, and by making such an evaluation graph according to the demand condition of each use and operation condition. On the other hand, it will be necessary to search for the factor that controls the output performance and the durability of the cell.

4. Conclusion

We have improved our past model, and presented the more realistic PEFC analysis model in this study. The PEFC

phenomenon was hardly measured experimentally, but our improved model can examine it with the numerical analysis in detail. The simulation shows that the cell output and the current density distribution increase by thinning the membrane and the GDL. In addition, the evaluation graph that became a help of those shape designs was made concerning the average current density and the current density distribution.

Acknowledgements

The present work was financially supported by the research and development of polymer electrolyte fuel cell from the New Energy and Industrial Technology Development Organization (NEDO), Japan.

References

[1] D.M. Bernardi, M.W. Verbrugge, Mathematical model of a gas diffusion electrode bonded to a polymer electrolyte, A.I. Ch. E.J. 37 (8) (1992) 1151–1163.
[2] D.M. Bernaldi, M.W. Verbrugge, A mathematical model of the solid–polymer–electrolyte fuel cell, J. Electrochem. Soc. 139 (9) (1992) 2477–2491.
[3] T.E. Springer, T.A. Zawodzinski, S. Gottesfeld, Polymer electrolyte fuel cell model, J. Electrochem. Soc. 138 (8) (1991) 2334–2342.
[4] T.F. Fuller, J. Newman, Water and thermal management in solid–polymer–electrolyte fuel cells, J. Electrochem. Soc. 140 (5) (1993) 1218–1225.
[5] T.V. Nguyen, R.E. White, A water and heat management model for proton-exchange-membrane fuel cells, J. Electrochem. Soc. 140 (8) (1993) 2178–2186.
[6] J.S. Yi, T.V. Nguyen, An along-the-channel model for proton exchange membrane fuel cells, J. Electrochem. Soc. 145 (4) (1998) 1149–1159.
[7] S. Um, C.Y. Wang, K.S. Chen, Computational fluid dynamics modeling of proton exchange membrane fuel cells, J. Electrochem. Soc. 147 (12) (2000) 4485–4493.
[8] Z.H. Wang, C.Y. Wang, K.S. Chen, Two-phase flow and transport in the air cathode of proton exchange membrane fuel cells, J. Power Sources 94 (2001) 40–50.
[9] S. Dutta, S. Shimpalee, J.W. Van Zee, Three-dimensional numerical simulation of straight channel PEM fuel cells, J. Appl. Electrochem. 30 (2000) 135–146.
[10] T. Berning, D. Lu, N. Djilali, Three-dimensional computational analysis of transport phenomena in a PEM fuel cell, J. Power Sources 106 (2002) 284–294.
[11] S. Mazumder, J.V. Cole, Rigorous 3-D mathematical modeling of PEM fuel cells model predictions with liquid water transport, J. Electrochem. 150 (11) (2003) 1510–1517.
[12] P.-W. Li, L. Schaefer, Q.-M. Wang, T. Zhang, M.K. Chyu, Multi-gas transportation and electrochemical performance of a polymer electrolyte fuel cell with complex flow channels, J. Power Sources 115 (2003) 90–100.
[13] S. Um, C.Y. Wang, Three-dimensional analysis of transport and electrochemical reactions in polymer electrolyte fuel cells, J. Power Sources 125 (2004) 40–51.
[14] T. Berning, N. Djilali, Three-dimensional computational analysis of transport phenomena in a PEM fuel cell—a parametric study, J. Power Sources 124 (2003) 440–452.
[15] G. Inoue, Y. Matsukuma, M. Minemoto, Evaluation of the optimal separator shape with reaction and flow analysis of polymer electrolyte fuel cell, J. Power Sources. 154 (2006) 18–34.